A CHANGE IN THE QUIESCENT X-RAY SPECTRUM OF THE NEUTRON STAR LOW-MASS X-RAY BINARY MXB 1659−29

E. M. CACKETT[1], E. F. BROWN[2], A. CUMMING[3], N. DEGENAAR[4], J. K. FRIDRIKSSON[5],
J. HOMAN[6], J. M. MILLER[4], AND R. WIJNANDS[5]

[1] Department of Physics and Astronomy, Wayne State University, 666 W. Hancock Street, Detroit, MI 48201, USA; ecackett@wayne.edu
[2] Department of Physics and Astronomy, National Superconducting Cyclotron Laboratory,
and the Joint Institute for Nuclear Astrophysics, Michigan State University, East Lansing, MI 48824, USA
[3] Department of Physics, McGill University, 3600 rue University, Montreal, QC H3A 2T8, Canada
[4] Department of Astronomy, University of Michigan, 500 Church Street, Ann Arbor, MI 48109-1042, USA
[5] Astronomical Institute "Anton Pannekoek", University of Amsterdam, Science Park 904, 1098-XH Amsterdam, The Netherlands
[6] Kavli Institute for Astrophysics and Space Research, Massachusetts Institute of Technology, 70 Vassar Street, Cambridge, MA 02139, USA

ABSTRACT

The quasi-persistent neutron star low-mass X-ray binary MXB 1659−29 went into quiescence in 2001, and we have followed its quiescent X-ray evolution since. Observations over the first 4 yr showed a rapid drop in flux and temperature of the neutron star atmosphere, interpreted as cooling of the neutron star crust which had been heated during the 2.5 yr outburst. However, observations taken approximately 1400 and 2400 days into quiescence were consistent with each other, suggesting the crust had reached thermal equilibrium with the core. Here we present a new *Chandra* observation of MXB 1659−29 taken 11 yr into quiescence and 4 yr since the last *Chandra* observation. This new observation shows an unexpected factor of ∼3 drop in count rate and change in spectral shape since the last observation, which cannot be explained simply by continued cooling. Two possible scenarios are that either the neutron star temperature has remained unchanged and there has been an increase in the column density, or, alternatively the neutron star temperature has dropped precipitously and the spectrum is now dominated by a power-law component. The first scenario may be possible given that MXB 1659−29 is a near edge-on system, and an increase in column density could be due to build-up of material in, and a thickening of, a truncated accretion disk during quiescence. But, a large change in disk height may not be plausible if standard accretion disk theory holds during quiescence. Alternatively, the disk may be precessing, leading to a higher column density during this latest observation.

Key words: stars: neutron – X-rays: binaries – X-rays: individual (MXB 1659−29)

Online-only material: color figures

1. INTRODUCTION

Neutron stars in transient low-mass X-ray binaries are expected to be hot thermal emitters during quiescence due to pycnonuclear reactions (Haensel & Zdunik 1990) occurring in the deep crust caused by compression during outburst (Brown et al. 1998). The crust, heated during outburst, is then expected to thermally relax once the outburst ends, cooling back into thermal equilibrium with the core (Ushomirsky & Rutledge 2001; Rutledge et al. 2002b). This should be particularly noticeable in quasi-persistent transients whose outbursts last years, rather than the more typical weeks to months. In 2001, two such quasi-persistent transients (KS 1731−260 and MXB 1659−29) went into quiescence (Wijnands et al. 2001, 2003), with both showing a significant drop in X-ray flux over the first few years after the end of their outbursts (Wijnands et al. 2002, 2004; Cackett et al. 2006, 2008, 2010). The observed decrease in X-ray flux is consistent with cooling of an accretion-heated neutron star crust. The rate of cooling and the final temperature when cooling stops allow us to put constraints on the structure of the crust and state of the core (Shternin et al. 2007; Brown & Cumming 2009). Such crustal cooling has now been observed in four additional sources (Degenaar et al. 2009, 2011a, 2011b; Degenaar & Wijnands 2011; Fridriksson et al. 2010, 2011; Díaz Trigo et al. 2011; J. Homan et al., in preparation), showing a variety of cooling timescales and temperatures.

Here, we present a new *Chandra* observation of MXB 1659−29 taken in 2012 July, approximately 4 yr after the last *Chandra* observation and almost 11 yr into quiescence. The first quiescent observation of MXB 1659−29 took place about 1 month into quiescence, finding a thermally dominated spectrum significantly brighter than a *ROSAT* upper limit from the 1990s (Wijnands et al. 2003). Follow-up monitoring showed that MXB 1659−29 cooled rapidly, displaying a factor of 7–9 decrease in X-ray flux in the first 1.5 yr (Wijnands et al. 2004), and a factor of approximately 25 decrease in the first 4 yr (Cackett et al. 2006). A further *Chandra* observation 6.6 yr into quiescence showed that the flux decrease had stopped, indicating the crust was likely back in thermal equilibrium with the core (Cackett et al. 2008). In this paper, we discuss a new observation of MXB 1659−29 where we find a significant drop in flux and a change in its spectrum since the previous observation that cannot simply be explained by continued crustal cooling.

2. DATA REDUCTION AND ANALYSIS

We observed MXB 1659−29 with *Chandra* for approximately 96 ks at the beginning of 2012 July. This observation was split into two segments. The first (ObsID: 13711) began on 2012 July 5, lasting 62.2 ks while the second (ObsID: 14453) began on 2012 July 8, lasting 33.6 ks. The ACIS-S instrument was operated using the FAINT data mode, with the source at the nominal aim point. The data were reduced using the most recent *Chandra*
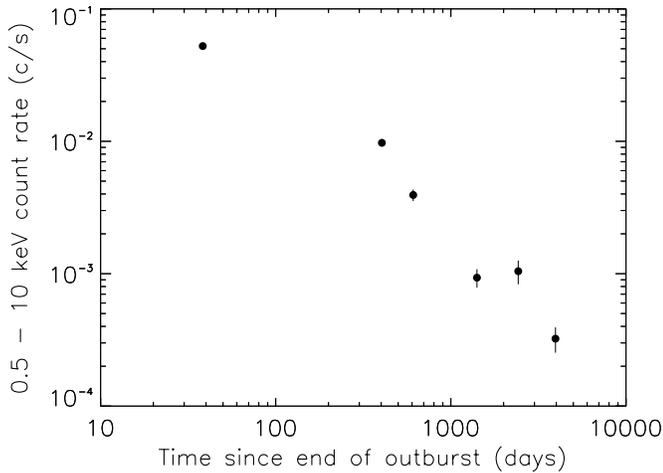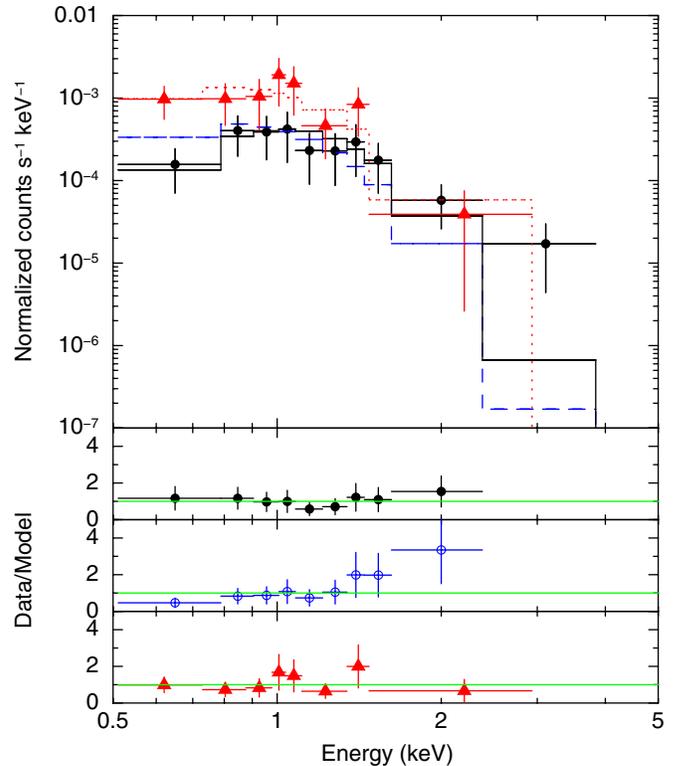
Figure 1. Count rate lightcurve of MXB 1659−29 as seen during the *Chandra* quiescent observations. Error bars are plotted for all points, but for the first points they are smaller than the symbols.

Figure 2. Top panel: *Chandra* spectra of MXB 1659−29. Black circles are from the most recent 2012 observation (ObsID: 13711 and 14453) where the two segments have been added together and rebinned for the purposes of plotting. The red triangles are from the preceding 2008 *Chandra* observation (ObsID: 8984) taken approximately 1500 days earlier. A significant difference below about 1.5 keV can be seen. The black solid line is the best-fitting absorbed neutron star atmosphere model when N_H is a free parameter, while the blue dashed line is when N_H is fixed to the previous value. The red dotted line is the best-fitting absorbed neutron star atmosphere model to ObsID 8984. There is no significant detection above 4 keV for either observation. Bottom three panels: these panels show the ratio of the data to the model. The top ratio panel (black filled circles) shows the ratio of the 2012 data to the model with N_H free (the solid black line in the spectrum panel), while the middle ratio panel (blue open circles) shows the ratio of the 2012 data to the model with N_H fixed (the dashed blue line in the spectrum panel). Note that the highest energy bin (approx. 2.5–3.5 keV) in these two panels has a ratio of greater than 10 and therefore cannot be seen in this figure. The bottom ratio panel (red triangles) shows the ratio of the 2008 data to the best-fitting absorbed neutron star atmosphere model (red dotted line in the spectrum panel.)

(A color version of this figure is available in the online journal.)

software (CIAO ver. 4.5). We used the `chandra_repro` tool to reprocess the data with the most recent calibration at the time of the analysis (CALDB ver. 4.5.5.1). We checked for background flaring and found none. A circular source extraction region of radius 3″ and an annular background extraction region with inner radius of 7″ and outer radius of 22″ were used. The source and background spectra and associated response files were extracted using the `specextract` tool.

MXB 1659−29 is a binary system viewed close to edge-on and thus regular X-ray eclipses have been seen from this source during outburst (Cominsky & Wood 1984, 1989) and quiescence (Wijnands et al. 2003). The eclipses last for 900 s and occur at the orbital period of 7.1 hr (Oosterbroek et al. 2001). Here, the source count rate is too low for us to be able to see eclipses, as well as to clearly distinguish between individual source and background photons. Therefore, as we have done with previous *Chandra* observations, we used the ephemeris of Oosterbroek et al. (2001) to determine the times of eclipses during our observation and manually reduce the effective exposure time to compensate for this. Two eclipses should have occurred during the first segment and one during the second; therefore, we reduced the source exposure times by 1800 s and 900 s giving corrected exposure times of 60.4 ks and 32.7 ks, respectively (the background exposure times remain unchanged). The average background-subtracted 0.5–10 keV count rate over the two exposures is $(3.2\pm0.7)\times10^{-4}$ counts s^{-1} (note that uncertainties quoted here and throughout the paper are at the 1σ level). The first exposure has a background-subtracted 0.5–10 keV count rate of $(3.8\pm0.9)\times10^{-4}$ counts s^{-1}, while the second exposure has $(2.1\pm1.0)\times10^{-4}$ counts s^{-1}, thus both segments have a marginally consistent count rate.

In Figure 1 we compare the count rate of this new observation with the previous six *Chandra* observations (see Cackett et al. 2008, and references therein). Note that we have averaged the count rate from ObsID 5469 and 6337 as the observations were performed only 17 days apart over 1000 days after the end of the outburst. The count rate of the 2012 observation shows a significant drop from the previous (2008) observation, dropping by a factor of three from $(1.0\pm0.2)\times10^{-3}$ counts s^{-1}, an approximately 3σ difference. Also note that both segments independently show a significant count rate drop compared to the last observation, suggesting that the drop is not a statistical

fluctuation. From Figure 1 it is interesting to speculate whether the penultimate observation was anomalously high or whether the latest observation shows an unexpected drop. Next we detail the spectral analysis to try and answer this question.

2.1. Spectral Analysis

In order to investigate the change between the observation in 2008 and 2012 we compare the spectra from these two observations. As can be seen in Figure 2, the most recent observation (black) is significantly fainter compared to the 2008 observation (red) below 1–1.5 keV. To determine whether this can be explained simply by cooling of the neutron star surface we fit the 2012 observation with an absorbed neutron star atmosphere. In fitting these data, we fit the spectra from the two segments (ObsID: 13711 and 14453) simultaneously, with all model parameters the same for the two segments. All fitting is performed with XSPEC version 12 (Arnaud 1996). The specific model we fit is phabs×nsa. We use the neutron star atmosphere model nsa for

ease of comparison with our previous analysis in Cackett et al. (2006) and Cackett et al. (2008). We fix the neutron star radius at 10 km, neutron star mass at 1.4 $M_\odot$ and assume a distance of 10 kpc, which gives an nsa normalization of 1×10^{-8} pc^{-2} (see Cackett et al. 2008 for a discussion on the choice of distance and its effects). Furthermore, we also assume that the equivalent hydrogen column density, $N_{\rm H}$, remains the same between the observations, fixing it to the value from Cackett et al. (2008) of 2.0×10^{21} cm^{-2}. Given the low number of counts we cannot bin the spectra to the minimum number of counts required for use of χ^2 statistics. We therefore use the C-statistic within XSPEC to fit the spectra which are binned to a minimum of 1 count per bin. Note that in the figures we show spectra that have been rebinned for plotting purpose, using the XSPEC command "setplot rebin 1.6 100". While this is a somewhat arbitrary choice, it allows for enough spectral bins to show the shape of the spectrum.
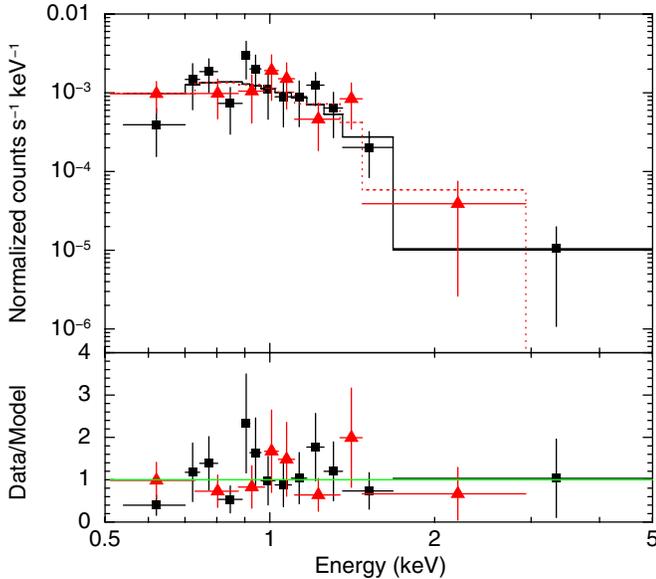
Fitting this simple absorbed neutron star atmosphere model in the 0.5–7 keV range we get a best-fitting effective temperature at infinity of $kT_{\rm eff}^\infty = 49 \pm 2$ eV. However, the model overpredicts the count rate below 0.8 keV and underpredicts it above about 1.5 keV, as can be seen in the ratio of the data to the model in Figure 2 (blue circles). For comparison, the 2008 observation has $kT_{\rm eff}^\infty = 56 \pm 2$ eV. If, however, we allow the $N_{\rm H}$ to be a free parameter an increased value is found as would be expected given the overprediction of the flux below 1 keV from the previous model. This model leads to $N_{\rm H} = (4.7 \pm 1.3) \times 10^{21}$ cm^{-2} and $kT_{\rm eff}^\infty = 55 \pm 3$ eV. This temperature is consistent with the 2008 observation. Note that if we let the $N_{\rm H}$ value be different for each of the two 2012 segments we get consistent values; however, note that the much shorter second segment has very few counts and thus is not very constraining.

When using the C-statistic, there is not a straightforward reliable way to determine the goodness of fit or comparing whether one model is an improvement over another. We therefore adopt the posterior predictive p-value (ppp) test (Protassov et al. 2002; Hurkett et al. 2008) in order to assess whether one model fits significantly better than another. This is a Monte Carlo based test to see whether the observed improvement in the C-statistic between two different models is significant or not. For instance, we can compare the fit with the neutron star atmosphere model with $N_{\rm H}$ fixed with the fit with the neutron star atmosphere model with $N_{\rm H}$ free. Let us call these model 1 and model 2 respectively for the sake of this discussion. In the ppp test we simulate 1000 sets of two spectra (one spectrum corresponding to ObsID 13711 and one corresponding to ObsID 14453) using the best fitting model 1. In simulating the spectra, the parameters for the model are randomly drawn using the covariance matrix of the best fit as well as using the exposures and background spectra from the real observation. These 1000 sets of simulated spectra are then fit with both model 1 and model 2 and the best-fitting C-statistic determined for each model. We then calculate the difference in the best-fitting C-statistic between model 1 and model 2 (ΔC), and define the posterior predictive distribution as the distribution of ΔC values. The ppp value is then calculated by comparing the fraction of instances where the simulated ΔC value is greater than the observed value. For the case comparing the neutron star atmosphere model with $N_{\rm H}$ fixed with the fit with the neutron star atmosphere model with $N_{\rm H}$ free, we find that only 13 instances out of 1000 simulations showed a ΔC value larger than observed, therefore indicating that the model with $N_{\rm H}$ free is better than with $N_{\rm H}$ fixed at the 98.7% confidence level ($1 - 13/1000 = 0.987$).

Trying an alternative model completely, we fit an absorbed power law, with the $N_{\rm H}$ fixed at 2.0×10^{21} cm^{-2}. This gives a power-law index of $\Gamma = 2.9 \pm 0.5$. This power-law index is softer than would be seen usually in quiescent systems where accretion is ongoing (e.g., Cen X-4; Cackett et al. 2010). A ppp test comparing the power-law fit with the neutron star atmosphere fit with $N_{\rm H}$ fixed at the old value shows that the power law is better at the 99.9% level (more than 3σ) while comparing the power law with the neutron star atmosphere fit with $N_{\rm H}$ free shows that the power law is better at the 94.3% confidence level (a little less than 2σ). Finally, we also test what happens if we try and fit an absorbed neutron star atmosphere plus power-law model. This is motivated by the fact that the neutron star atmosphere model alone underpredicts the count rate above 2 keV (see Figure 2) possibly indicating the presence of a power-law component in addition to a neutron star atmosphere component. However, the power law dominates and the temperature of the neutron star atmosphere goes as low as possible, indicating that two model components is beyond the quality of the data. Alternatively, if we fix the power-law index at $\Gamma = 1.5$ and the $N_{\rm H}$ at the previous value (2.0×10^{21} cm^{-2}), then we find that the power law contributes 58% to the unabsorbed 0.5–10 keV flux and we get $kT_{\rm eff}^\infty = 45 \pm 3$ eV. If instead we fix $\Gamma = 2$ we then get a power-law fraction of 62% and $kT_{\rm eff}^\infty = 43 \pm 5$ eV. Thus, we cannot rule out a significant contribution from a power-law component. A ppp test comparing the neutron star atmosphere with $N_{\rm H}$ free with the neutron star atmosphere plus power-law model (with $\Gamma = 1.5$) indicates an improvement from adding the power law at the 94.7% confidence level. Note that if we fit all the previous observations with an absorbed neutron star atmosphere plus power-law model we find that the power-law component is not statistically required in any of them. If we also compare the simple power-law fit with the neutron star atmosphere plus power-law fit (with $\Gamma = 1.5$), we find they give equivalent fits with the ppp test indicating no significant improvement (49.9% confidence level).

We also compare the 2008 observation with the two observations closely spaced in time taken in 2005 in order to test whether the 2008 observation is anomalously high rather than the 2012 observation being anomalously low. We show a comparison of the two sets of observations in Figure 3, where we have added the spectra together from ObsID 5469 and 6337 given that they were taken only 17 days apart and have similar spectral shapes. This figure shows that both observations from 2005 and 2008 look very similar, and hence, it appears to be the 2012 observation that is anomalously low. The 2008 observation does not appear to show clear signs of a strong power-law component which might be expected from signs of ongoing accretion as would be indicated by significant emission above 3 keV. An increased temperature caused by ongoing accretion (see, for instance, temperature increases in XTE J1701−462 during sporadic accretion events; Fridriksson et al. 2011) is also not observed. But, the 2012 observation does appear to be harder than a simple neutron star atmosphere, and is better fit by a simple power law (a power law gives an improvement over the best neutron star atmosphere model at the 94.3% confidence level). This may possibly indicate some cooling between 2012 and 2008, though the extremely low count rate limits what constraints we can get on the temperature from the 2012 observation when fitting with a neutron star atmosphere plus power-law model.

Finally, we rule out that there has been a build-up of contaminant on the optical blocking filters (see, e.g., Marshall

Figure 3. Top panel: *Chandra* spectra of MXB 1659−29 with best-fitting absorbed neutron star atmosphere model. Black squares are from the combined 2005 observations (ObsID: 5964 and 6337) while the red triangles are from the 2008 observation (ObsID: 8984). The spectra are clearly consistent with one another. Bottom panel: the ratio of the data to the best-fitting model shown in the upper panel.

(A color version of this figure is available in the online journal.)

et al. 2004) between ObsIDs 8984 and 13711/14453 that is yet to be modeled and included in the detector responses. We extract the spectrum from nearby source CXOU J170205.9−295619 from ObsIDs 8984 and 13711/14453 using `specextract`. We find that this source has a constant count rate and spectral shape (absorbed power law) between the observations. In particular it shows no signs of any changes below 1.5 keV.

3. DISCUSSION

We have continued to monitor the spectrum of the crustal cooling source MXB 1659−29 since it entered into quiescence in 2001. Here, we have presented a new *Chandra* observation from 2012 July (almost 11 yr into quiescence). While initial monitoring of MXB 1659−29 showed that it cooled rapidly over the first few years in quiescence, the observation from 2008 indicated that cooling had appeared to halt (Cackett et al. 2008). However, this new observation shows an unexpected drop in count rate by a factor of three since the preceding *Chandra* observation performed 4 yr earlier. Spectral analysis comparing the new 2012 data with the 2008 spectrum shows that the 2012 spectrum is systematically below the 2008 spectrum at energies less than about 1–1.5 keV (Figure 2).

We are left with several options to explain the count rate drop between the 2008 and 2012 observations. Firstly, the drop in count rate is not real, but a statistical outlier. However, note that the drop is at the 3σ level and that both separate pointings in 2012 show a similar count rate drop. Second, the neutron star has cooled slightly, but the N_H has remained constant. Third, the neutron star has remained at a constant temperature but the N_H has increased. Fourth, the neutron star temperature has dropped precipitously and the spectrum is now dominated by a (rather soft) power law. Option two is not favored based on spectral fitting—a model with temperature free and N_H remaining constant shows clear residuals (see Figure 2). Options three and four both give improved spectral fits. For

instance, the fit is improved (at the 98.7% confidence level) by fitting an absorbed neutron star atmosphere where the N_H has increased from 2.0×10^{21} cm^{-2} (Cackett et al. 2008) to $N_H = (4.7 \pm 1.3) \times 10^{21}$ cm^{-2} yet the neutron star temperature is consistent with remaining constant. Alternatively, the spectrum is well fit by an absorbed power law with index $\Gamma = 2.9 \pm 0.5$ with an unchanged N_H.

Let us first examine the possibility of an increase in column density. In this scenario, the neutron star is back in thermal equilibrium as we see that the temperature is consistent between the 2008 and 2012 observations. But, we need a physical motivation to explain the increase in column density—in most systems a change in column density would not be expected. However, MXB 1659−29 is a nearly edge-on system that shows eclipses both in outburst and quiescence. Models for the accretion disk during quiescence usually have the disk truncated at a few thousand Schwarzschild radii, essentially acting as a reservoir for material transferred from the companion star (e.g., Lasota 1996; Esin et al. 1997; Dubus et al. 2001). Material then builds up in the outer disk during quiescence until an outburst is triggered. At the time of the 2012 observation, MXB 1659−29 was almost 11 yr into quiescence. The previous known quiescent period for this object is 21 yr (in 't Zand et al. 1999). If MXB 1659−29 follows a similar pattern this time, then it is approximately half way through its quiescent period. We can speculate, then, that during quiescence the build-up of material could increase the scale height of the outer disk, leading to an increase in absorption. Under such a scenario, we might expect the absorbing column to further increase as quiescence progresses, which can be tested by future observations.

Considering standard accretion disk theory, however, a large change in scale height during quiescence is not expected. If we assume that the standard α disk holds during quiescence, then we can determine how the disk properties scale. In order that the truncated disk remains stable, and an outburst is not triggered, the temperature in the outer disk cannot rise by a large factor. Yet, for a given radius, the height of the disk scales as $c_s \sim \sqrt{T}$ (where c_s is the sound speed and T the temperature in the disk). Thus, a factor of two increase in temperature would only lead to a 40% increase in the disk height. Moreover, the temperature in quiescence is also likely to be colder than when in outburst, thus, a lower scale height would be expected in quiescence. Hence, if standard disk theory holds in quiescence a significant change in disk height may not be plausible.

An alternative explanation for the increase in column density is that the accretion disk could be precessing. In this scenario, during the 2012 observations our line of sight passes through more of the disk than in previous observations. Superorbital periods have been detected in at least 25 X-ray binaries (see Kotze & Charles 2012 and references therein). The two main mechanisms for superorbital periods are precession (Whitehurst & King 1991) or radiation-induced warping (Ogilvie & Dubus 2001), though see Kotze & Charles (2012) for suggestions of other possible mechanisms. During quiescence, irradiation of the outer disk will be many orders of magnitude less than during outburst, thus radiation-induced warping would not be expected. Precession, however, may occur when there is an extreme mass ratio when $M_2/M_1 \leqslant 0.25$–0.33 (Whitehurst & King 1991). MXB 1659−29 has a known optical counterpart (Wachter et al. 2000; Wijnands et al. 2003), which is thought to be a K0 star (Wachter & Smale 1998; Wachter et al. 2000). Such a companion, however, would not lead to the required mass ratio for precession. No significant detection of a superorbital

period has been reported for MXB 1659−29, though Kotze ([2012](#)) report a very marginal detection at the 1.2σ level at a period of about 350 days. Thus, we cannot completely rule out the possibility of precession, despite the mass ratio. In this precession scenario, we would more likely than not see a return to the previous column density in future observations, though this depends on the exact modulation timescale for the precession. We may also expect to have already seen some hints of this in previous data, but again, this depends on the precession period and the sparse sampling of X-ray observations we have may not be enough to have detected it.

We now consider the other possibility, that the spectrum is now dominated by a power-law component. This would require that the neutron star surface cooled dramatically between 2008 and 2012. Unfortunately, the data quality does not permit constraints on the neutron star temperature, as a second component (in addition to the power law) is not required by the data. But, if dominated by the power law then such a component could be due to low-level accretion during quiescence or alternative mechanisms. However, there is no sign of a strong power-law component in previous observations (see Figure 3), and, the 2008 and 2012 spectra are very similar above about 1.5 keV. Previous observations can be fit by a single absorbed power law, but such fits give a high power-law index, e.g., ObsID 8984 gives $\Gamma = 4.2 \pm 0.5$. Additionally, in the presence of low-level accretion one would expect a somewhat warmer neutron star component (e.g., Fridriksson et al. [2011](#)), while here we see a cooler one. Moreover, the photon index of approximately 3 is softer than other quiescent neutron stars, especially those that just display a power law and no clear thermal component, such as EXO 1745−248 (Wijnands et al. [2005](#)) and SAX J1808.4−3658 (Heinke et al. [2009](#)). Signatures of ongoing accretion might include sporadic variability in quiescence as has been seen in several other quiescent neutron stars (Campana et al. [1997](#), [2004](#); Rutledge et al. [2001](#), [2002a](#); Cackett et al. [2005](#), [2010](#), [2011](#); Fridriksson et al. [2011](#)), and could be seen via future observations.

If we consider that the spectrum is now power-law-dominated, then we must discuss the implications for crustal cooling. A significant drop in temperature cannot be reconciled with the crust cooling models of Brown & Cumming ([2009](#)). Even a modest drop to just 49 eV (as implied by the spectral fit with an absorbed neutron star atmosphere and fixed column density) causes the model to fit the 2005 and 2008 data points poorly, as we show in Figure 4. Page & Reddy ([2012](#)) do show a model (their Figure 12) which shows a further decline in temperature at late times. However, this model is calculated specifically for XTE J1701−462, which was accreting above the Eddington limit during an outburst of only 1.6 yr (Homan et al. [2007](#); Lin et al. [2009](#)). This high accretion rate for a comparatively short time leads to a crust temperature profile with two peaks—one near the surface, and one in the inner crust, with a dip in between. This leads to a cooling curve with an initial drop that plateaus (corresponding to the dip in the crust profile) and then has a second drop at late times. For a longer outburst at a lower accretion rate (as is the case for MXB 1659−29) the temperature profile of the crust should be flatter (without two separate peaks), and thus a second drop in temperature is not expected for MXB 1659−29.

In conclusion, we cannot definitively explain the cause of the drop in count rate between the 2008 and 2012 observation of MXB 1659−29. However, the possible scenarios predict different future behavior. The picture where material is building
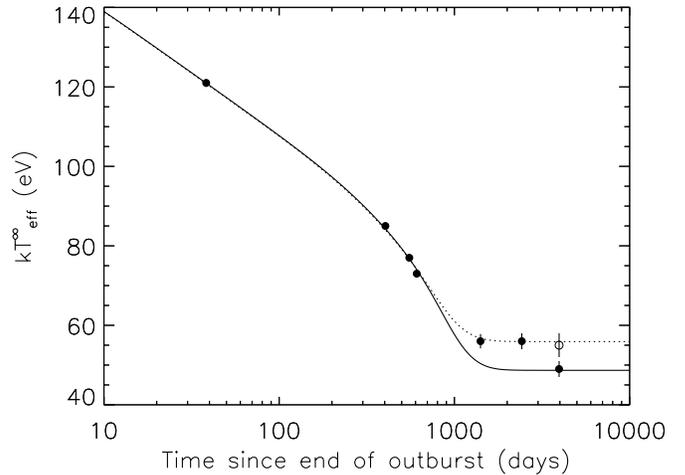
Figure 4. Theoretical cooling curves calculated using the model described in Brown & Cumming ([2009](#)) compared to the observed temperatures (Cackett et al. [2008](#); though note ObsIDs 5469 and 6337 have been averaged). The dotted line shows the best-fitting model from Brown & Cumming ([2009](#)), while the solid line shows the best-fitting model if a temperature of 49 eV is assumed for the 2012 observation (the fit with $N_{\rm H}$ fixed, filled circle). The additional point causes a poor fit at times between 1000 and 3000 days. Note that the final data point becomes consistent with the dotted line if the fit with $N_{\rm H}$ as a free parameter is used (open circle).

up in the outer disk and leading to an increase in absorption leads to the expectation that a further increase in column density could be seen in the future. In the precession scenario we would most likely expect $N_{\rm H}$ to return to its previous value in the future. Alternatively, the explanation involving low-level accretion and a much colder neutron star leads to the expectation of sporadic variability in quiescence. Future observations of MXB 1659−29 can test between these scenarios.

REFERENCES

Arnaud, K. A. 1996, in ASP Conf. Ser. 101, Astronomical Data Analysis Software and Systems V, ed. G. H. Jacoby & J. Barnes (San Francisco, CA: ASP), 17
Brown, E. F., Bildsten, L., & Rutledge, R. E. 1998, ApJL, 504, L95
Brown, E. F., & Cumming, A. 2009, ApJ, 698, 1020
Cackett, E. M., Brown, E. F., Cumming, A., et al. 2010, ApJL, 722, L137
Cackett, E. M., Fridriksson, J. K., Homan, J., Miller, J. M., & Wijnands, R. 2011, MNRAS, 414, 3006
Cackett, E. M., Wijnands, R., Heinke, C. O., et al. 2005, ApJ, 620, 922
Cackett, E. M., Wijnands, R., Linares, M., et al. 2006, MNRAS, 372, 479
Cackett, E. M., Wijnands, R., Miller, J. M., Brown, E. F., & Degenaar, N. 2008, ApJL, 687, L87
Campana, S., Israel, G. L., Stella, L., Gastaldello, F., & Mereghetti, S. 2004, ApJ, 601, 474
Campana, S., Mereghetti, S., Stella, L., & Colpi, M. 1997, A&A, 324, 941
Cominsky, L. R., & Wood, K. S. 1984, ApJ, 283, 765
Cominsky, L. R., & Wood, K. S. 1989, ApJ, 337, 485
Degenaar, N., Brown, E. F., & Wijnands, R. 2011a, MNRAS, 418, L152
Degenaar, N., & Wijnands, R. 2011, MNRAS, 414, L50

Degenaar, N., Wijnands, R., Wolff, M. T., et al. 2009, MNRAS, 396, L26
Degenaar, N., Wolff, M. T., Ray, P. S., et al. 2011b, MNRAS, 412, 1409
Díaz Trigo, M., Boirin, L., Costantini, E., Méndez, M., & Parmar, A. 2011, A&A, 528, A150
Dubus, G., Hameury, J.-M., & Lasota, J.-P. 2001, A&A, 373, 251
Esin, A. A., McClintock, J. E., & Narayan, R. 1997, ApJ, 489, 865
Fridriksson, J. K., Homan, J., Wijnands, R., et al. 2010, ApJ, 714, 270
Fridriksson, J. K., Homan, J., Wijnands, R., et al. 2011, ApJ, 736, 162
Haensel, P., & Zdunik, J. L. 1990, A&A, 227, 431
Heinke, C. O., Jonker, P. G., Wijnands, R., Deloye, C. J., & Taam, R. E. 2009, ApJ, 691, 1035
Homan, J., van der Klis, M., Wijnands, R., et al. 2007, ApJ, 656, 420
Hurkett, C. P., Vaughan, S., Osborne, J. P., et al. 2008, ApJ, 679, 587
in 't Zand, J., Heise, J., Smith, M. J. S., et al. 1999, IAUC, 7138, 1
Kotze, M. M. 2012, PhD thesis, Univ. Cape Town
Kotze, M. M., & Charles, P. A. 2012, MNRAS, 420, 1575
Lasota, J. P. 1996, in IAU Symp. 165, Compact Stars in Binaries, ed. J. van Paradijs, E. P. J. van den Heuvel, & E. Kuulkers (Dordrecht: Kluwer), 43
Lin, D., Remillard, R. A., & Homan, J. 2009, ApJ, 696, 1257
Marshall, H. L., Tennant, A., Grant, C. E., et al. 2004, Proc. SPIE, 5165, 497
Ogilvie, G. I., & Dubus, G. 2001, MNRAS, 320, 485
Oosterbroek, T., Parmar, A. N., Sidoli, L., in't Zand, J. J. M., & Heise, J. 2001, A&A, 376, 532
Page, D., & Reddy, S. 2012, in Neutron Star Crust, ed. C. A. Bertulani & J. Piekarewicz (Hauppauge, NY: Nova Science Publishers), in press
Protassov, R., van Dyk, D. A., Connors, A., Kashyap, V. L., & Siemiginowska, A. 2002, ApJ, 571, 545
Rutledge, R. E., Bildsten, L., Brown, E. F., Pavlov, G. G., & Zavlin, V. E. 2001, ApJ, 551, 921
Rutledge, R. E., Bildsten, L., Brown, E. F., Pavlov, G. G., & Zavlin, V. E. 2002a, ApJ, 577, 346
Rutledge, R. E., Bildsten, L., Brown, E. F., et al. 2002b, ApJ, 580, 413
Shternin, P. S., Yakovlev, D. G., Haensel, P., & Potekhin, A. Y. 2007, MNRAS, 382, L43
Ushomirsky, G., & Rutledge, R. E. 2001, MNRAS, 325, 1157
Wachter, S., & Smale, A. P. 1998, ApJL, 496, L21
Wachter, S., Smale, A. P., & Bailyn, C. 2000, ApJ, 534, 367
Whitehurst, R., & King, A. 1991, MNRAS, 249, 25
Wijnands, R., Guainazzi, M., van der Klis, M., & Méndez, M. 2002, ApJL, 573, L45
Wijnands, R., Heinke, C. O., Pooley, D., et al. 2005, ApJ, 618, 883
Wijnands, R., Homan, J., Miller, J. M., & Lewin, W. H. G. 2004, ApJL, 606, L61
Wijnands, R., Miller, J. M., Markwardt, C., Lewin, W. H. G., & van der Klis, M. 2001, ApJL, 560, L159
Wijnands, R., Nowak, M., Miller, J. M., et al. 2003, ApJ, 594, 952